Agricultural and Forest Meteorology 156 (2012) 65–74

Contents lists available at SciVerse ScienceDirect

Agricultural and Forest Meteorology

journal homepage: www.elsevier.com/locate/agrformet

Reflections on the surface energy imbalance problem

Ray Leuning[a,*], Eva van Gorsel[a], William J. Massman[b], Peter R. Isaac[c]

[a] CSIRO Marine and Atmospheric Research, P.O. Box 3023, Canberra, ACT 2601, Australia
[b] USDA - Forest Service, Rocky Mountain Research Station, 240 West Prospect, Fort Collins, CO 80526, USA
[c] School of Geography and Environmental Science, Monash University, Clayton, VIC 3800, Australia

ARTICLE INFO

Article history:
Received 13 September 2011
Received in revised form
26 November 2011
Accepted 9 December 2011

Keywords:
Energy balance closure
Eddy covariance flux measurements
Micrometeorology
Advective flux divergence

ABSTRACT

The 'energy imbalance problem' in micrometeorology arises because at most flux measurement sites the sum of eddy fluxes of sensible and latent heat ($H + \lambda E$) is less than the available energy (A). Either eddy fluxes are underestimated or A is overestimated. Reasons for the imbalance are: (1) a failure to satisfy the fundamental assumption of one-dimensional transport that is necessary for measurements on a single tower to represent spatially-averaged fluxes to/from the underlying surface, and (2) measurement errors in eddy fluxes, net radiation and changes in energy storage in soils, air and biomass below the measurement height. Radiometer errors are unlikely to overestimate A significantly, but phase lags caused by incorrect estimates of the energy storage terms can explain why $H + \lambda E$ systematically underestimates A at half-hourly time scales. Energy closure is observed at only 8% of flux sites in the La Thuile dataset (http://www.fluxdata.org/DataInfo/default.aspx) with half-hourly averages but this increases to 45% of sites using 24 h averages because energy entering the soil, air and biomass in the morning is returned in the afternoon and evening. Unrealistically large and positive horizontal gradients in temperature and humidity are needed for advective flux divergences to explain the energy imbalance at half-hourly time scales. Imbalances between $H + \lambda E$ and A still occur in daily averages but the small residual energy imbalances are explicable by horizontal and vertical advective flux divergences. Systematic underestimates of the vertical heat flux also occur if horizontal $u'T'$ covariances contaminate the vertical $w'T'$ signal due to incorrect coordinate rotations. Closure of the energy balance is possible at half-hourly time scales by careful attention to all sources of measurement and data processing errors in the eddy covariance system and by accurate measurement of net radiation and every energy storage term needed to calculate available energy.

1. Introduction

Because it violates the law of conservation of energy, the failure of the sum of eddy fluxes of sensible and latent heat ($H + \lambda E$) to equal the available energy (A) is a long-standing problem in micrometeorology (Twine et al., 2000; Wilson et al., 2002; Oncley et al., 2007; Foken, 2008; Franssen et al., 2010). Available energy is net absorbed all-wave radiation minus the changes in energy storage in soils and in the air column and biomass below the measurement height. The summary by Wilson et al. (2002) of data from 50 site-years of data from 22 FLUXNET sites showed that half-hourly averages $H + \lambda E$ underestimated A at most sites by around 20%. Many reasons for lack of energy budget closure have been proposed, including: (1) a failure to meet the fundamental assumptions underlying eddy covariance measurements (see below); (2) errors in radiation measurements (Halldin and Lindroth, 1992); (3) incorrect accounting for storage of energy in soil, air column and vegetation (Meyers and Hollinger, 2004; Haverd et al., 2007; Lindroth et al., 2010); (4) advective flux divergence caused by complex terrain or heterogeneities in vegetation cover (Katul et al., 2006); (5) low-frequency, mesoscale transport (Foken, 2008); (6) inadequate averaging periods to capture low frequency contributions to net exchange (Finnigan et al., 2003); (7) loss of high frequency covariance due to line-averaging and instrument separation (Moore, 1986) or by sampling air through tubing before analysis (Leuning and Judd, 1996; Massman, 1991, 2000; Massman and Ibrom, 2008); and (8) choice of coordinate systems (Finnigan, 2004).

It is important to resolve the 'energy closure problem' because among many applications, data from the international FLUXNET network of flux stations (Baldocchi et al., 2001) are being used to test, parameterize and constrain outputs of land surface schemes in climate models (see review by Williams et al., 2009), and to develop empirical, global maps of fluxes of water vapor and CO_2 (Jung et al., 2009). Systematic errors in eddy flux measurements will propagate directly into the resultant data products and possibly compromise such studies.

* Corresponding author. Tel.: +61 2 6246 5557.
E-mail address: ray.leuning@csiro.au (R. Leuning).

0168-1923/$ – see front matter © 2011 Elsevier B.V. All rights reserved.
doi:10.1016/j.agrformet.2011.12.002

Much has been written about errors in eddy covariance measurements due to the design of instruments, the measurement system and data processing (above references, Foken and Wichura, 1996; Mauder et al., 2007). Here we focus on the conservation equations for mass and energy of a notional control volume surrounding a flux station to examine likely micrometeorological explanations for the lack of energy closure. We first clarify the assumptions required to ensure that measurements on a single tower are representative of fluxes from the underlying surface, followed by a brief review of errors in measurement and data processing of eddy fluxes. Correct measurements of the available energy require knowing both net radiation and the changes in energy stored in soils, the air column and in aboveground biomass for every half-hourly averaging period typically used by the flux measurement community. Phase lags caused by incorrect estimates of the storage terms are shown to be a major reason why the sum of sensible and latent heat fluxes systematically underestimates the available energy at these time scales. Small imbalances between $H+\lambda E$ and A still occur in daily averages but are explicable by advective flux divergence which can transport energy to or from a control volume surrounding a flux station. Horizontal temperature gradients needed to account for the advective flux divergence are estimated using a simple analysis. The effects of incorrect coordinate rotation and radiation measurements on the energy imbalance problem are also discussed.

2. Conservation equations

Following Leuning (2004), the conservation equation for a scalar quantity χ in a control volume (CV) of height h and length of side L is given by

$$\begin{aligned}\bar{F} &= \bar{F}(0) + \frac{1}{L^2}\int_0^L\int_0^L\int_0^h \bar{S}dzdxdy = \frac{1}{L^2}\int_0^L\int_0^L\int_0^h \overline{c_d}\frac{\partial\overline{\chi}}{\partial t}dxdydz \\ &+ \frac{1}{L^2}\int_0^L\int_0^L\int_0^h \left[\overline{u}\overline{c_d}\frac{\partial\overline{\chi}}{\partial x} + \overline{v}\overline{c_d}\frac{\partial\overline{\chi}}{\partial y} + \overline{w}\overline{c_d}\frac{\partial\overline{\chi}}{\partial z}\right]dxdydz \\ &+ \frac{1}{L^2}\int_0^L\int_0^L\int_0^h \left[\frac{\partial\overline{c_d}\overline{u'\chi'}}{\partial x} + \frac{\partial\overline{c_d}\overline{v'\chi'}}{\partial y} + \frac{\partial\overline{c_d}\overline{w'\chi'}}{\partial z}\right]dxdydz \end{aligned} \quad (1)$$

Here $\bar{F}$ is the time- and space-average flux density (mol m^{-2} s^{-1}) of χ between the surface and the atmosphere, $\bar{F}(0)$ is its flux density at the ground and $\bar{S}$ is the source strength per unit volume (mol m^{-3} s^{-1}). The quantities u, v, w (m s^{-1}) are the wind vector components in the x, y, z directions orthogonal to the walls of the CV, t is time, c_d is the concentration of dry air (mol m^{-3}). Standard Reynold's notation is used to express the instantaneous value of a quantity as the sum of the mean and fluctuations about the mean, and the overbar represents the time averaging operator. The first term in the second equality of Eq. (1) is the rate of change of χ in the CV, the second term is the sum of mean horizontal and vertical flux divergences and the third term is the sum of eddy flux divergences. Triple correlations are assumed to be small and are neglected. Eq. (1) also applies to the flux of sensible heat if $\overline{c_d}\chi$ is replaced by $\overline{\rho_a}c_pT$, where $\overline{\rho_a}$ is air density (kg m^{-3}), c_p is the specific heat of moist air at constant pressure (J kg^{-1} K^{-1}) and T is air temperature.

Neglecting the horizontal eddy flux divergences and assuming the scalar intensities measured on a single mast are representative of the control volume, Eq. (1) becomes

$$\bar{F} = \underbrace{\overline{c_d}\overline{w'\chi'}}_{\text{I}} + \underbrace{\int_0^h \overline{c_d}\frac{\partial\overline{\chi}}{\partial t}dz}_{\text{II}} + \frac{1}{L^2}\int_0^L\int_0^L\int_0^h \left[\underbrace{\overline{u}\overline{c_d}\frac{\partial\overline{\chi}}{\partial x}}_{\text{III}} + \underbrace{\overline{v}\overline{c_d}\frac{\partial\overline{\chi}}{\partial y}}_{\text{IV}} + \underbrace{\overline{w}\overline{c_d}\frac{\partial\overline{\chi}}{\partial z}}_{\text{V}}\right]dxdydz \quad (2)$$

The eddy flux (I), change in storage (II) and vertical advective flux divergence (V) can be measured using instruments on a single mast but it is not possible to measure the horizontal flux divergences (III and IV) with such an arrangement. It is thus necessary to locate the flux station in flat, horizontally homogeneous terrain where the advective flux divergence terms can be neglected a priori, since only then can terms I and II in Eq. (2) be used to measure correctly the net exchange of χ between the surface and the atmosphere. With these additional restrictions the conservation equation is given by the sum of an eddy covariance term and a storage term:

$$\bar{F} = \overline{c_d}\overline{w'\chi'} + \int_0^h \overline{c_d}\frac{\partial\overline{\chi}}{\partial t}dz \quad (3)$$

Inability to satisfy the highly demanding criterion of horizontal homogeneity in both surface fluxes and air flow is likely to be a major cause of incorrect measurements at many flux stations.

Conservation of energy requires that the sum of sensible (H) and latent heat fluxes (λE) should equal the available energy (A), and the degree to which this criterion is satisfied is often used to assess the accuracy of eddy covariance measurements of sensible and latent heat fluxes which are defined as

$$\overline{H} = \overline{\rho_a}c_p\overline{w'T'} \quad \text{and} \quad \lambda\overline{E} = \lambda M_w\overline{c_d}\overline{w'\chi_w'} \quad (4)$$

Here λ is the latent heat of evaporation (J kg^{-1}), M_w is the molecular mass of water (kg mol^{-1}) and χ_w is the mol fraction of water vapor relative to dry air (mol mol^{-1}).

In the absence of advective flux divergence, the available energy for flat, homogeneous surfaces is given by

$$\overline{A} = \overline{R_n} - \overline{G_0} - \overline{J_a} - \overline{J_b} - \overline{J_w} - \overline{J_p} \quad (5)$$

(W m^{-2}), where $\overline{R_n}$ is the net all-wave radiation absorbed by the vegetation and soil, $\overline{G_0}$ is the flux of heat through the soil surface. $\overline{J_a}$ and $\overline{J_b}$ are the changes in heat storage associated with temperature changes in the moist air column and in the biomass below the flux measurement height, $\overline{J_w}$ is the latent heat associated with the change in water vapor stored in the air column and $\overline{J_p}$ is the radiant energy absorbed in photosynthesis or heat released by respiration. The storage fluxes in the air column and biomass are given by

$$\overline{J_a} = \int_0^h \overline{\rho_a}c_p\frac{\overline{dT}}{dt}dz, \quad \overline{J_w} = \int_0^h \lambda M_w\overline{c_d}\frac{\overline{d\chi_w}}{dt}dz,$$

$$\overline{J_b} = \int_0^h m_bc_b\frac{\overline{d\left\langle T_b\right\rangle}}{dt}dz, \quad (6)$$

where m_b is the mass of wood and leaves above ground, c_b is the specific heat capacity of these components, while $\left\langle T_b\right\rangle$ is a suitably averaged biomass temperature (Haverd et al., 2007). $\overline{J_p}$ is estimated as, $\overline{J_p} = -\alpha_p\overline{F_{CO_2}}$ where $\alpha_p = 0.469$ (J µmol^{-1}, Blanken et al., 1997) and $\overline{F_{CO_2}}$ is the flux of CO_2 (µmol m^{-2} s^{-1}).

Soil heat flux is typically measured at some depth z_m, below the surface and following Fuchs and Tanner (1968) it is then necessary to estimate the heat flux at the surface G_0, using

$$G_0 = G_{z_m} + \int_0^{z_m} C_s\frac{dT_s}{dt}dz = G_{z_m} + J_s, \quad (7)$$

in which the second term accounts for the storage flux in the soil layer above the heat flux plates. The volumetric heat capacity of the soil C_s is a function of soil moisture content and because both this and soil temperature T_s can vary strongly close to the surface, it is especially difficult to estimate the storage term accurately for bare soil or surfaces with sparse vegetation cover. An alternative approach is to use harmonic analysis (van Wijk and de Vries, 1963, p. 133) to calculate the 'damping depth' of the heat wave from the amplitudes, ΔT, of the sinusoidal, diurnal temperature waves measured at depths z_1 and z_m (m, positive downwards):

$$z_D = \frac{z_m - z_1}{\ln(\Delta T_1/\Delta T_m)}, \quad z_m > z_1 \tag{8}$$

The heat flux at the surface G_0, is then calculated from G_{z_m} using

$$G_0 = G_{z_m} \exp(z_m/z_D) \tag{9}$$

where G_0 leads G_{z_m} by $\Delta t = 24z_m/(2\pi z_D)$ hours. It is important to bury the soil heat flux plates below the greatest expected depth of the evaporating front to avoid confounding energy used in evaporation with the change in energy stored in the soil (Buchan, 1989; Heitman et al., 2010). Inserting the heat flux plates at the surface as done by Heusinkveld et al. (2004) is thus not recommended.

The energy closure problem is characterized by $H + \lambda E < A$, so either the eddy fluxes of H and or λE are underestimated or the available energy is overestimated (Wilson et al., 2002; Foken, 2008), but only if the advective flux divergence terms in Eq. (2) are negligible. Before considering the flux divergence terms, we first examine the contributions of uncertainties in measurements in the eddy fluxes and the available energy to the energy closure problem at hourly and daily timescales.

3. Uncertainties in eddy covariance measurements

Much has been written on the instrumentation and data processing needed to make accurate eddy covariance measurements of mass and energy fluxes and only a brief summary is presented here. Authoritative texts include *Atmospheric Boundary Layer Flows* (Kaimal and Finnigan, 1994), the *Handbook of Micrometeorology*, edited by Lee, Massman and Law (2004), and *Eddy Covariance: A Practical Guide to Measurement and Data Analysis*, edited by Aubinet et al. (2011). Burba and Anderson (2010) provide a useful best-practice guide to making eddy covariance measurements.

A typical eddy covariance system consists of a sonic anemometer placed at some height h above the surface of interest to measure the wind vector components u, v, w and the sonic temperature T_{son}, in combination with additional instrument(s) to measure concentrations of water vapor, CO_2 and other trace gases using open- or closed-path analysers. Correct measurements require translation of velocity components from sonic anemometer coordinates into the orthogonal set used to define the CV in the above conservation equations, and conversion of the sonic temperature into true air temperature (Kaimal and Businger, 1963; Schotanus et al., 1983, Liu et al., 2001). Careful calibration of all instruments against well-defined standards is clearly necessary but this can be difficult to achieve when the instruments are in the field. A comprehensive maintenance program is also necessary to minimize measurement uncertainties.

It is essential to regard the instrument array as a system whose performance may be inferior to that of its individual parts. Almost every component of an eddy covariance system causes fluxes to be underestimated. Underestimates of the high-frequency component of covariances required to calculate H and λE (Eq. (4)) occur because of finite sampling path-lengths of sonic anemometers and open-path gas analysers as well separation between instruments. Algorithms to correct for these errors have been summarized by Moore (1986), Massman (2000), Massman and Clement (2004), Spank and Bernhofer (2008) and references therein. Corrections are particularly large under stable atmospheric conditions and when $d_{inst}/(h - d) > 0.1$, where d_{inst} is the diameter of a notional sphere inscribing the instrument array, h is the measurement height and d is the zero-plane displacement height. Without suitable correction, loss of high-frequency covariance will be most severe for instruments placed 1–2 m above pastures and crops (Leuning and Moncrieff, 1990; Leuning and King, 1992). Closed-path analysers have been used to measure concentrations of water vapor and other traces gases because they can be readily calibrated in situ and because there is less loss of data compared to open-path analysers that is caused by rain, mist and snow. Unfortunately, flow of air through tubing causes loss of high-frequency concentration fluctuations and hence loss of $w'\chi'_w$ covariance, even after allowing for the time delay between when the air enters the sampling tubing and when it passes through the analyser. This problem is particularly severe for water vapor which readily adsorbs and desorbs on tubing walls and particle filters (Ibrom et al., 2007; Massman and Ibrom, 2008; Mammarella et al., 2009). These effects can be minimized by having high flow rates to ensure turbulent flow in the tubing, short tubing lengths and by measuring temperature and pressure fluctuations in addition to concentrations in the analysis cell (Leuning, 2004; Clement et al., 2009). The relative merits of open- and closed-path gas analysers is discussed by Leuning and Judd (1996), Massman and Clement (2004), Massman (2004) and Haslwanter et al. (2009).

Eddy fluxes of H and λE can also be underestimated by using averaging periods that are too short to capture the low-frequency contributions to the covariances (Finnigan et al., 2003). These errors increase as the measurement height increases because larger, low-frequency eddies then contribute significantly to the fluxes. An averaging period of 30 min is used at most eddy flux sites globally but it is essential to test whether longer averaging periods are needed at a given site to ensure there are no low-frequency losses in the covariances. Increasing the averaging time from 15 mins to 1 h increased H by ~8% and λE by 12% measured at 71 m above the 40 m forest at Tumbarumba, with similar increases at the Manaus forest (Finnigan et al., 2003). Smaller increases are expected when measurements are made at lower heights where turbulent transport is dominated by smaller, high-frequency eddies.

Once the appropriate low-and high-frequency corrections have been applied it is necessary to apply the theory of Webb et al. (1980) as confirmed by Leuning (2004, 2007) and Massman (2004) to account for spurious fluctuations in water vapor and trace gas concentrations measured by open-path instruments due to fluctuations in temperature and water vapor itself. Typically, water vapor fluxes must be increased by 5% of H (Webb et al., 1980), but the corrections can be very large for CO_2 and other trace gas fluxes, especially when sensible heat fluxes are large (Leuning et al., 1982; Kondo and Tsukamoto, 2008). Propagation of measurement errors causes uncertainties to increase from sensible heat, to water vapor and then to CO_2 and other trace gases.

4. Uncertainties in measurement of available energy

There is little evidence that all radiometers used by the flux measurement community systematically overestimate R_n even though many researchers have found inconsistencies between various makes and designs of instruments (Halldin and Lindroth, 1992; Kustas et al., 1998; Brotzge and Duchon, 2000; Kohsiek et al., 2007; Blonquist et al., 2009). Kohsiek et al. (2007) compared the performance of several radiometers from different manufacturers and concluded that the maximum error in net radiation was 25 W m^{-2} (5%) during the day and 10 W m^{-2} at night. They found that deviations in R_n between a reference, 4-component radiation system and a CNR1 (Kipp and Zonen, www.kippzonen.com) and a Schulze-Däke instrument was within 20 W m^{-2}, but a Q*7.1 radiometer (REBS, Seattle, WA) showed deficits of 30 W m^{-2}. Michel et al. (2008) observed that a CNR1 net radiometer, with factory-default calibration coefficients, overestimated hourly-average R_n by <15 W m^{-2} compared to $R_{n,\text{ref}}$ measured with high-quality reference instruments for $0 < R_{n,\text{ref}} < 600$ W m^{-2}. There were no significant differences between R_n and $R_{n,\text{ref}}$ in the daily-means provided there was no dew on the test instrument. Brotzge and Duchon (2000) compared seven NR-Lite (Kipp and Zonen) instruments, a CNR1, a Q*7.1 and an Eppley PSP-PIR system (http://www.eppleylab.com/) and observed differences of <±20 W m^{-2} in the average daily net radiation. Similar results were obtained by Blonquist et al. (2009) for CNR1 and NR-Lite instruments but a Q*7.1 radiometer underestimated daytime hourly R_n by ~8%. These and other published results show there is variability between radiometers but errors in radiation measurements are unlikely to account for the systematic overestimation of >100 W m^{-2} needed to explain the energy imbalances often observed at half-hourly time scales.

5. Radiation measurement: sloping terrain

Care must be taken in estimating the available energy in sloping terrain. Radiation instruments are mounted horizontally but net radiation depends on the slope and aspect of the surface, especially during daytime; e.g. a south facing slope in the northern hemisphere will absorb more solar radiation than will be measured by a horizontal instrument. Theory presented by Olmo et al. (1999) and Matzinger et al. (2003) can be used to estimate global irradiance and net all-wave radiation on inclined surfaces from irradiances measured with horizontal instruments.

Olmo et al. (1999) present a simple model (see Appendix A) to estimate the global irradiance on an inclined surface, G_ψ, given measurements in the horizontal plane, G_H. The ratio G_ψ/G_H calculated using Eq. (A1) is shown in Fig. 1 for two values of the clearness index k_t (0.4, 0.8) as a function of solar zenith angle θ_s, for a 0°–30° range of ψ, the angle between the normal to the inclined surface and the direction of the sun. The cosine of θ_s is also shown for the response of an ideal, horizontal radiation sensor. Global radiation intercepted by an inclined surface exceeds that on the horizontal when $\psi > 20°$ and $\theta_s < 25°$, and at these angles G_ψ/G_H is greater for clear skies ($k_t = 0.8$) when direct radiation dominates radiation absorption than for overcast conditions ($k_t = 0.4$). For $\theta_s > 25°$ G_ψ/G_H decreases more rapidly when $k_t = 0.8$ than when $k_t = 0.4$.

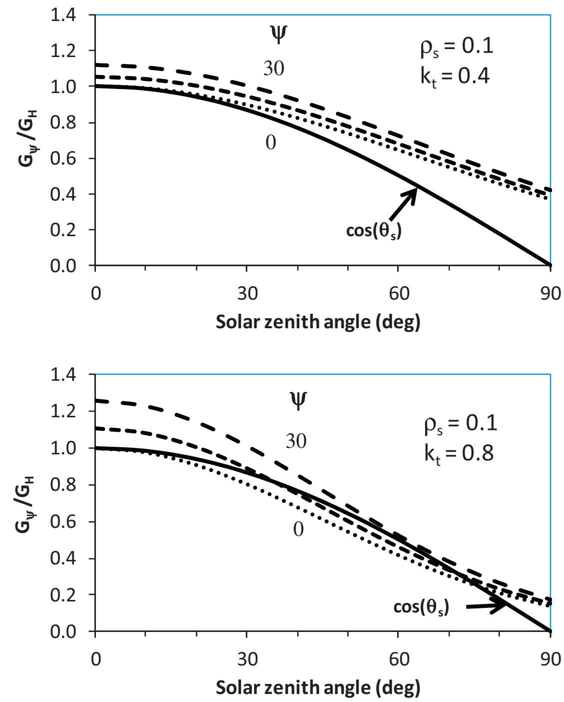

Fig. 1. The ratio of global radiation on an inclined surface to that on a horizontal surface (G_ψ/G_H) as a function of solar zenith angle θ_s for $\psi = 0°$, 20° and 30°. ρ_s is the short-wave albedo and k_t is the clearness index (the ratio of global to extraterrestrial horizontal irradiance). The thick black line is cos(θ_s), the cosine response of an ideal horizontal radiometer.

6. Storage terms – soil, vegetation, air

Soil heat fluxes are commonly measured using heat flux plates buried at several centimetres to avoid confounding the energy flux that heats or cools the soil with that used to evaporate water at the drying front several millimetres below the surface (Buchan, 1989). The heat flux varies with depth and soil temperatures must be measured to account for changes in energy stored above the flux plate, the so-called combination method (Eq. (7)) and/or by harmonic analysis of the diurnal temperature wave with depth (Eqs. (8) and (9)). Failure to account for the storage term can cause errors in G_0 of 10–200 W m^{-2} for bare soils or under sparse vegetation (Heusinkveld et al., 2004). It is difficult to make accurate measurements of the storage term when soil heat capacity varies with depth due to variation in soil moisture content and/or because of large spatial and temporal variability in soil heat fluxes across a measurement site. Heat flux plates are typically 50–100 mm in diameter and because they sample a tiny area compared to that of the eddy covariance measurements (typically >10^4 m^2), multiple measurements are needed to estimate the mean soil heat flux accurately. Useful reviews of various methods to measure soil heat fluxes are given by Massman (1993), Sauer and Horton (2005) and Ochsner et al. (2007). Early theoretical analyses of heat transport into soils were presented by Philip (1961) and van Wijk and de Vries (1963).

Heat fluxes into soils are generally small below dense and/or tall vegetation but then storage fluxes to and from the biomass need to be considered. For crops and grasses it may be sufficiently accurate to calculate the storage term using infrared thermometry (Meyers and Hollinger, 2004) or by equating the rate of change in biomass temperature with that of the air within the canopy, but this will not be suitable for trees with their large biomass. Change in heat storage can be calculated using the third expression in Eq. (6) when bole temperatures are measured and the heat capacities of the bark and wood are known (Lindroth et al., 2010). When biomass temperatures are not measured, changes in heat storage in tree trunks can be estimated using theory presented by Haverd et al. (2007) which uses measured changes in air temperature and calculated radiation absorbed by tree trunks As an example, estimated heat storage fluxes peaked at ~60 W m^{-2} in a 40 m tall evergreen forest at Tumbarumba (Leuning et al., 2005) and subtraction of this term from the net radiation improved the hourly energy budget closure from 90% without J_b to 101% with it (Haverd et al., 2007). Inclusion of the changes in biomass heat storage significantly improved half-hourly energy balance closure for maize and soybean crops (Meyers and Hollinger, 2004) and for a forest (Lindroth et al., 2010).

The storage terms $\overline{J_a}$ and $\overline{J_w}$ associated with temperature and humidity changes in the air column below the measurement height h can be ignored over pastures and crops but should be included when measurements are made over tall vegetation. A positive heat storage flux of 47 W m^{-2} around dawn was calculated by Haverd et al. (2007) with a similar negative value at dusk, corresponding to times when the canopy air temperature changes most rapidly.

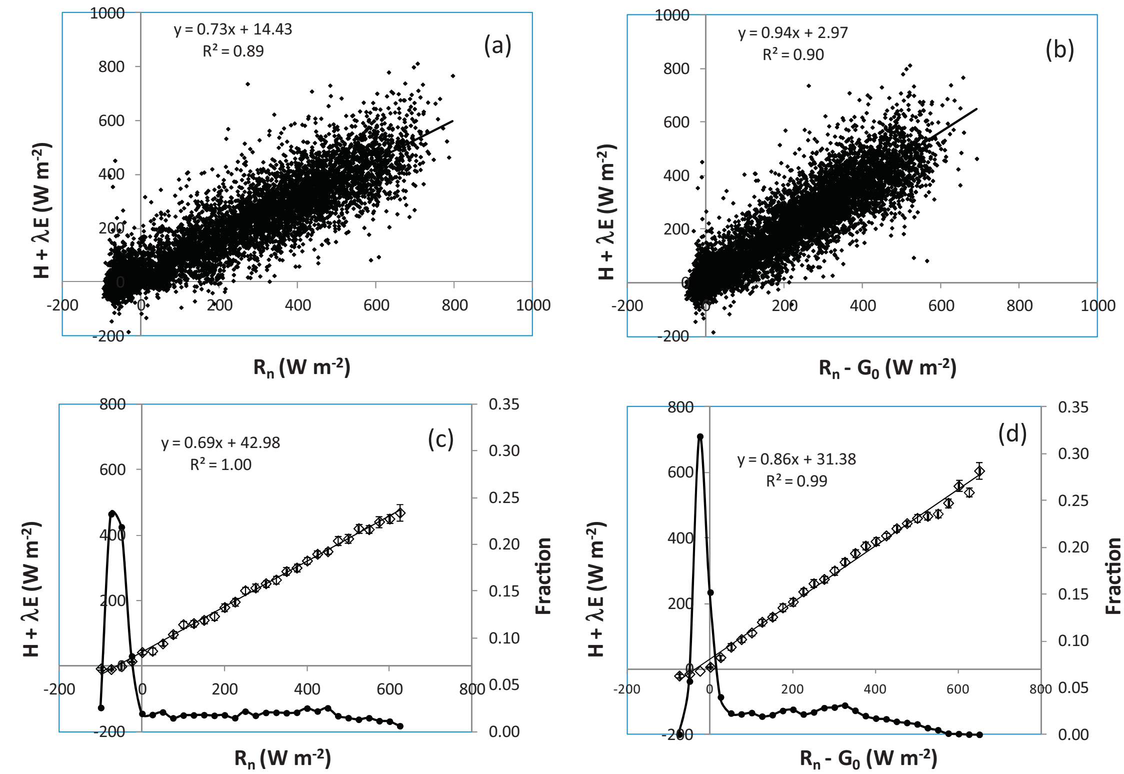

Fig. 2. Scatter plots of $H + \lambda E$ versus (a) R_n and (b) $R_n - G_0$ for hourly-average measurements at Virginia Park. Panels (c) and (d) show corresponding averages and 2× standard errors for R_n and $R_n - G_0$ in bins of 25 W m^{-2}. The fraction of data in each bin is also shown.

Contributions by $\overline{J_w}$ were typically <20 W m^{-2}. Again, including these terms in Eq. (5) was necessary to close the hourly energy budgets at Tumbarumba.

7. Comparison of $H + \lambda E$ versus A

It is clear that disagreement between $H + \lambda E$ and A will occur unless all terms in Eqs. (4) and (5) are evaluated accurately for each half-hourly averaging period typically used by the flux measurement community. An example of errors introduced by ignoring the storage terms is shown in Fig. 2 using ~12200 hourly-average measurements at Virginia Park (VP), a wet-dry season tropical savanna ecosystem in northern Queensland (Leuning et al., 2005). The tree cover at this site is sparse and soil heat fluxes are an important component of the energy budget. When G_0 is ignored (Fig. 2a), the slope of the linear regression of $H + \lambda E$ versus R_n is 0.702 and the intercept is 31.5 W m^{-2}. This slope increases to 0.924 and the intercept decreases to 7.0 W m^{-2} when estimates of G_0 obtained using Eq. (7) are subtracted from R_n each hour (Fig. 2b). Similar results were obtained when G_0 was estimated using Eqs. (8) and (9) (data not shown). The improvement in energy closure is seen more clearly in the lower two panels where the hourly data have been averaged into 25 W m^2 bins of R_n and $R_n - G_0$, respectively. Approximately 24% of the data points occur when $R_n < 0$ and 32% for $R_n - G_0 < 0$ W m^{-2}. $H + \lambda E$ appears to asymptote to zero rather than continuing along the regression line obtained from positive fluxes but removal of these data from the regression analysis does not significantly improve the apparent lack of energy closure.

Failure to account for the storage terms correctly for each hour invariably leads to a regression slope less than unity. This is shown in Fig. 3 where the hourly data from VP have been combined into a composite 24 h day. R_n leads $H + \lambda E$ in the morning, peaks at a higher value around noon, lags it late in the afternoon and is less than $H + \lambda E$ at night. These phase shifts lead to the hysteresis loop shown in Fig. 3c and a linear regression forced through the hourly data has a slope less than one. This is a general result as shown by Gao et al. (2010) who used theory for heat transport in soils to demonstrate that phase shifts between H, λE and G_0 leads to a lack of energy closure at hourly timescales. Subtracting G_0 from R_n greatly improves the agreement between $R_n - G_0$ and $H + \lambda E$ in the diurnal plot (Fig. 3b) and almost eliminates the hysteresis loop (Fig. 3d). The agreement is not perfect because the corresponding slopes and intercepts in Fig. 2d are still less than one and greater than zero, respectively.

Lack of energy closure at hourly time scales may thus simply be caused by inaccurate estimates of the storage terms. This leads to the question whether the energy balance can be closed on daily timescales on the premise that energy stored in the soil, air and biomass during the morning is released locally in the afternoon and evening. A suitable averaging period is thus from one midnight to the next. The success of this approach is seen in Fig. 4 when applied to the VP dataset, where there is excellent agreement between 24 h averages of $H + \lambda E$ and of both R_n and $R_n - G_0$. Daily averages for three other Australian datasets also result in better energy closure than hourly averages but at the cost of slightly lower R^2 values, whether or not the regressions are forced through the origin (Table 1). In contrast, using daily averages did not improve energy closure at the GLEES coniferous forest site in Wyoming during 2010 (Table 1). Similar results were obtained for 2007, 2008 and 2009 (not shown). The GLEES site is in complex terrain and advective flux divergences due to drainage flows may negate the assumption that energy stored in soil, air and biomass in the morning is released locally later in the day.

To see whether averaging over 24 h improves agreement between $H + \lambda E$ and A more generally, we analysed 948 site-years of data from the La Thuile dataset (http://www.fluxdata.org/DataInfo/default.aspx). Linear regressions of $H + \lambda E$ versus $R_n - G_0$

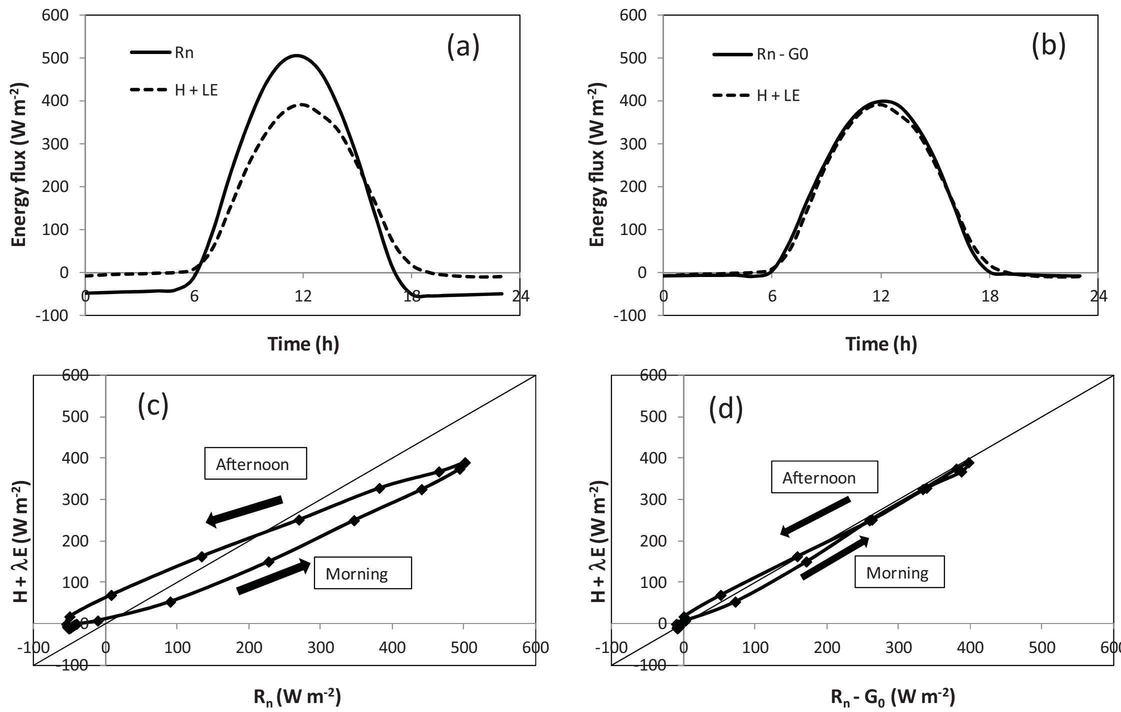

Fig. 3. Composite diurnal plots of (a) R_n and $H + \lambda E$, and (b) $R_n - G_0$ and $H + \lambda E$ at Virginia Park. Corresponding hysteresis curves are shown in (c) and (d).

were obtained for 594 and 439 site-years for half-hourly and daily averages, respectively. All sites with regression slopes <0.45 or >1.35 were eliminated from the analysis because close inspection showed either flux or radiation data from those sites were seriously in error. While measurement errors undoubtedly exist in the remaining dataset, our objective is to test whether 24 h averaging decreases the apparent lack of energy closure despite such errors. Frequency distributions of regression slopes forced through the origin are shown in Fig. 5 for half-hourly and daily averages. The median slope is 0.75 for the half-hourly averages, increasing to 0.90 for daily averages. Slopes ≥1 were found for <8% of sites when half-hourly averages were used but this increased to 45% of sites using daily averages. Restricting the analysis to sites with >50 days having all 48 half hours of data did not change the distributions (not shown). It is now necessary to explain both the under- and over-estimates of $H + \lambda E$ compared to $R_n - G_0$ on daily timescales.

8. Discussion: causes for discrepancies

8.1. Incorrect coordinate system

Components of the wind vector are output as an orthogonal set of velocities in the coordinate system of the sonic anemometer. The instruments are usually installed horizontally rather than being aligned with the mean stream lines of air flow over the surface, so it is necessary to rotate the velocity vectors mathematically to force the mean vertical and crosswind velocities to zero. This eliminates the corresponding mean advective flux divergence terms IV and V in Eq. (2) while term III is zero for horizontally homogeneous flows over uniform surfaces. The planar fit approach of Wilczak et al. (2001) uses long-term wind vector measurements to define a single coordinate system, while other researchers rotate the wind vectors to force $\overline{w} = 0$ for each averaging period. Further discussion of coordinate systems can be found in Finnigan et al. (2003) and Finnigan (2004).

Another reason to carefully define the co-ordinate system is to avoid contamination of the vertical $\overline{w'T'}$ covariance with some fraction f of the horizontal eddy flux $\overline{u'T'}$. This always has a sign opposite to $\overline{w'T'}$ (Stull, 1988, Ch. 9), and for the example of data from the Otway site (Fig. 6a), we observe a slope of $a \approx -2$ for positive (upward) heat fluxes and $a \approx -4$ for negative (downward) fluxes. A simple analysis results in

$$b = \frac{1}{1 - af} \tag{10}$$

where $b(\leq 1)$ is the slope of the measured $\overline{w'T'}$ covariance versus the true value. To a first approximation b is the slope of the linear regression of $H + \lambda E$ versus A. Fig. 6b shows that as the tilt angle ($\arcsin f$) increases from 0 to 3 degrees, b decreases from 1.0 to 0.91 when $a = -2$ and from 1.0 to 0.82 when $a = -4$. It is clear that even small a misalignment of the coordinate system causes the true vertical sensible heat fluxes to be underestimated significantly.

Table 1
Statistics for linear regression of $H + \lambda E$ (y) versus $R_n - G_0$ (x) at hourly and daily timescales. The intercept has units of W m^{-2}.

Site	Description	Hourly		Daily		Hourly			Daily		
		Slope[a]	R^2	Slope[a]	R^2	Slope	Intercept	R^2	Slope	Intercept	R^2
Otway (2007–2008)	Pasture	0.866	0.967	0.949	0.943	0.840	11.1	0.970	0.864	9.0	0.956
Sturt Plains (2009)	Tropical grassland	0.861	0.853	1.075	0.862	0.793	30.5	0.884	0.962	12.2	0.875
Tumbarumba (2001–2005)	Evergreen forest	0.904	0.838	1.182	0.850	0.853	31.2	0.854	0.986	28.0	0.898
Virginia Park (2001–2004)	Tropical savanna	0.944	0.876	0.973	0.835	0.924	7.0	0.877	0.873	12.6	0.848
GLEES (2010)	Conifer forest	0.727	0.914	0.747	0.846	0.718	6.2	0.915	0.688	9.8	0.854

[a] Slope forced through origin.

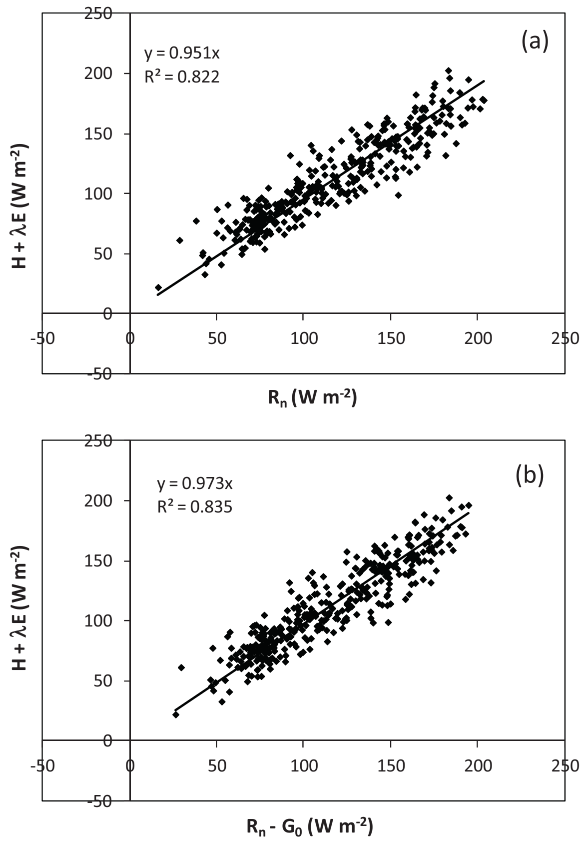

Fig. 4. Scatter plots of $H + \lambda E$ versus (a) R_n and (b) $R_n - G_0$ for daily-average measurements at Virginia Park.

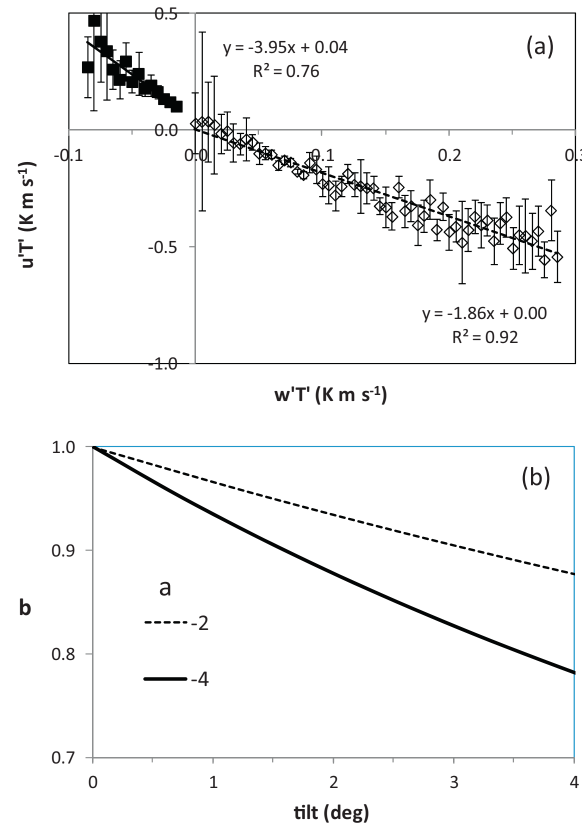

Fig. 6. (a) Relationship between horizontal covariance $u'T'$ and vertical covariance $w'T'$ at the Otway flux station. (b) The effect of tilt angle on the slope b, of the measured $w'T'$ covariance versus the true covariance. To a first approximation b is the slope of $H + \lambda E$ versus A.

Similar arguments apply to the latent heat flux. One solution to this cross-contamination may be to choose a coordinate system that maximizes the $\overline{w'T'}$ and $\overline{w'\chi'_w}$ covariances rather than the current practise of forcing $\overline{w} = 0$. This may produce unstable results and further work is needed to test this suggestion.

Inaccuracies in estimating heat storage in the soil, air and biomass at half-hourly time scales and incorrect coordinate rotation both lead to underestimation of the true heat and water vapor fluxes. Increasing the averaging time to 24 h reduces errors in the storage terms but cannot correct for cross-contamination between horizontal and vertical eddy fluxes. We next consider the role of advective flux divergence in the energy closure problem.

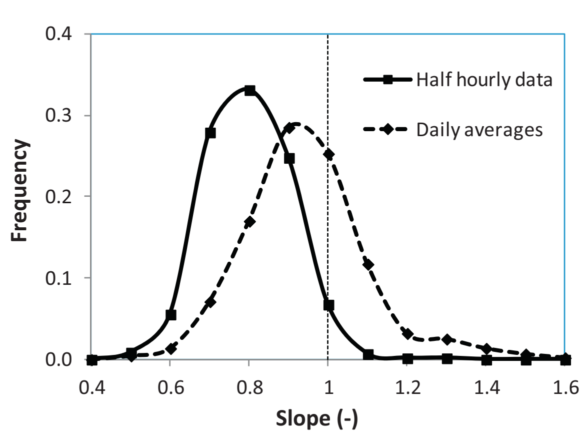

Fig. 5. Frequency distributions for the slope of $H + \lambda E$ versus $R_n - G_0$ (forced through zero) for half-hourly and daily averages of measurements reported in the La Thuile datset.

9. Advective flux divergence

In the La Thuile dataset the slope of $H + \lambda E$ versus A is ≥ 1 for only 8% of sites when half-hourly data are used (Fig. 5). Advective flux divergence would need to be systematically negative (energy export from the CV) to explain the lack of energy closure at almost every site, but this is unlikely because the flux divergence can be positive or negative depending on the sign of the scalar gradient terms in Eq. (2). However, advective flux divergence does provide a plausible explanation when the averaging time is increased to 24 h, since this raises the median slope of $H + \lambda E$ versus A to 0.90 (i.e., a smaller energy imbalance) and increases the proportion of sites with regression slopes ≥ 1 to 45% (Fig. 5). Deviation from the ideal slope of one can now be due to advective flux divergence importing or exporting sensible and latent heat from the CV.

Horizontal and vertical advective flux divergence will occur at sites located in heterogeneous landscapes and/or complex topography due to flow divergence/convergence and recirculating flows (Katul et al., 2006; Foken, 2008; Harman and Finnigan, 2010), thereby violating the assumptions required for Eq. (3) to be valid (Simple Cartesian coordinate systems do not apply in complex terrain). Advective flux divergence occurs when stable atmospheric conditions within plant canopies decouple turbulent exchange of heat and mass between the vegetation and the atmosphere (van Gorsel et al., 2011). Drainage flows within canopies on hillsides under stable conditions can cause the advective flux divergence terms in Eq. (2) to dominate the eddy flux and storage terms (van Gorsel et al., 2007; Yi et al., 2008).

Large-eddy simulations (LES) by Kanda et al. (2004) support the suggestion of Foken (2008) and others that low-frequency mesoscale circulations due to landscape heterogeneity can explain

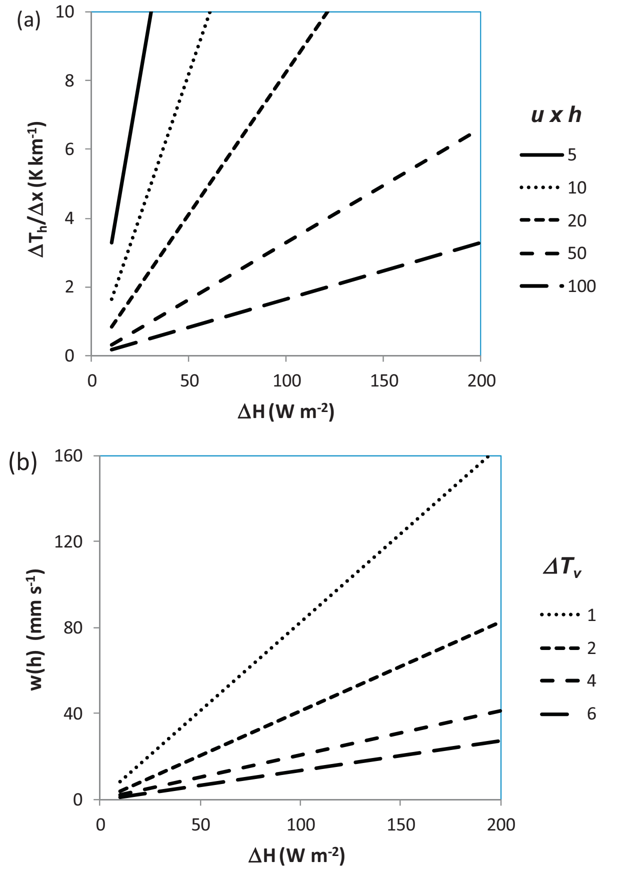

Fig. 7. (a) The absolute magnitude of horizontal temperature gradients $\Delta T/\Delta x$ needed to account for advective flux divergence errors ΔH as a function of the product of the mean horizontal wind speed $(\overline{u})$ at the measurement height h. (b) The absolute magnitude of the vertical wind speed $\overline{w}(h)$ needed to account for advective flux divergence errors ΔH as a function of the vertical temperature difference $\Delta\overline{T_v}$.

the lack of energy closure due to what Steinfeld et al. (2007) call 'locally non-vanishing mean vertical advection due to turbulent organized structures (TOS)'. The strength of the TOS and thus the magnitude of the energy imbalance depends on measurement height, the horizontal mean wind and atmospheric stability. However, these structures do not resolve the imbalance problem because they account for imbalances that are an order of magnitude smaller than those observed at typical eddy flux sites (Steinfeld et al., 2007). As noted by Finnigan (1999), horizontal and vertical advective flux divergences occur together but often with opposite signs, thereby diminishing the net effect of these flux divergences.

To estimate the magnitude of the horizontal temperature gradient needed to account for a given horizontal flux divergence of sensible heat $\Delta\overline{H}$, we note that

$$\Delta\overline{H} = \overline{\rho}c_p \int_0^h \overline{u}\frac{d\overline{T}}{dx}dz \approx \overline{\rho}c_p h \frac{\overline{u_h}}{2}\frac{\Delta\overline{T}}{\Delta x}, \tag{11}$$

where mean wind speed between the ground and h has been approximated by $\overline{u_h}/2$. A similar expression can be written for the flux divergence for water vapor. Thus

$$\frac{\Delta\overline{T}}{\Delta x} \approx \frac{2\Delta\overline{H}}{\overline{\rho}c_p\overline{u_h}h}, \quad \frac{\Delta\overline{\chi_w}}{\Delta x} \approx \frac{2\Delta\overline{\lambda E}}{\overline{c_d}\lambda M_w\overline{u_h}h} \tag{12}$$

Errors in H of 50–100 W m^{-2} are common at the hourly time scale and Fig. 7a shows that unrealistically large temperature gradients of 5–10° K km^{-1} are needed to account for such values of $\Delta\overline{H}$ when $\overline{u_h}h < 20\,m^2\,s^{-1}$. Errors in λE of 50–100 W m^{-2} also require unrealistically large horizontal gradients in χ_w.

Vertical advective flux divergence of sensible heat can be estimated using the approximation proposed by Lee (1998)

$$\Delta\overline{H} = \overline{\rho}c_p \int_0^h \overline{w}\frac{\partial\overline{T}}{\partial t}dz \approx \overline{\rho}c_p\overline{w}(h)\left[\overline{T}(h) - \frac{1}{h}\int_0^h \overline{T}dz\right] \tag{13}$$

The term in square brackets is the difference in temperature at h and the average temperature of the air layer below h and writing this as $\Delta\overline{T_v}$ we obtain

$$\overline{w}(h) = \frac{\Delta\overline{H}}{\overline{\rho}c_p\Delta\overline{T_v}}, \tag{14}$$

which is the mean vertical velocity needed to account for the advective flux divergence error. Estimates of $\overline{w}(h)$ are shown as a function of $\Delta\overline{H}$ and $\Delta\overline{T_v}$ in Fig. 7b. These velocities are quite small (<160 mm s^{-1}) but again, the values of $\Delta\overline{T_v}$ needed to account for $\Delta\overline{H}$ are unrealistically large, especially during daytime when the energy balance closure problem is most apparent (Fig. 2).

We have shown that the large discrepancies in hourly-average fluxes can be explained, at least partially, by inaccurate estimates of heat storage in the soil and biomass (Fig. 3) or by incorrect coordinate rotation (Fig. 6). Unrealistically large horizontal and vertical gradients in temperature and humidity are needed to account for the apparent energy imbalance and the true magnitude of $\Delta\overline{H} + \Delta\overline{\lambda E}$ is likely to be of order 20–30 W m^{-2} if the storage terms are evaluated correctly. Such advective flux divergence errors can be positive or negative and require only plausibly small horizontal temperature and humidity gradients and/or small mean vertical velocities and vertical temperature gradients to account for the 'missing' energy.

10. Conclusions

Half-hourly measurements of sensible and latent heat fluxes appear to systematically underestimate the available energy at most eddy covariance sites, but a substantial part of this underestimate can be explained by phase lags caused by incorrect estimates of the energy storage in soils, air and biomass below the measurement height. Unrealistically large and positive horizontal gradients in temperature and humidity are needed for advective flux divergences to explain the energy imbalance at half-hourly time scales. With half-hourly averages, energy closure is observed at only 8% of flux sites in the La Thiuile dataset but this increases to 45% using 24 h averages because energy entering the soil and biomass in the morning is returned in the afternoon and evening. Imbalances between $H + \lambda E$ and A still occur in the daily averages but the small residual energy imbalances are explicable by advective flux divergence transporting energy to or from the control volume surrounding a flux station. Systematic underestimates of the vertical heat flux also occur if horizontal $u'T'$ covariances contaminate the vertical $w'T'$ signal due to incorrect coordinate rotations. Radiation measured by horizontal sensors must be adjusted to correctly account for net radiation absorbed by inclined surfaces. Closure of the energy balance is possible at half-hourly time scales by careful attention to all sources of measurement and data processing errors in the eddy covariance system and by accurate determination of all components of the available energy. Selection of horizontally homogeneous sites is necessary to satisfy the assumptions of one-dimensional transport underpinning eddy covariance measurements on single towers.

Acknowledgements

We gratefully acknowledge the excellent technical assistance of Steve Zegelin, Dale Hughes, for installing and maintaining the

Otway, Tumbarumba and Virginia flux stations, and thank Darren Hocking for Sturt Plains and John Franks for the GLEES site. Ian Harman and Vanessa Haverd plus two anonymous referees are thanked for valuable comments on the manuscript. Our analysis of the La Thuile dataset is only possible through the dedication and generosity of a very large number of researchers across the globe who have made their data available to the general research community. It is hoped that this paper repays their generosity is some small measure. This work was supported by the Australian Climate Change Program (RL and E v G).

Appendix A. Global irradiance on inclined surfaces

Olmo et al. (1999) present a simple model to estimate the global irradiance on an inclined surface, G_ψ, given measurements in the horizontal plane, G_H. Their Eq. (6) is

$$G_\psi = G_H \exp\left[-k_t(\psi^2 - \theta_s^2)\right]\left[1 + \rho_s \sin^2(\psi/2)\right] \tag{A1}$$

where the clearness index k_t is the ratio of measured global to calculated extraterrestrial horizontal irradiance, ρ_s is the surface albedo, θ_s is the solar zenith angle and ψ is the angle between the normal to the inclined surface and the direction of the sun. All angles are expressed in radians.

Following Goudriaan and van Laar (1994), the solar elevation angle β is calculated using

$$\sin\,\beta_s = \sin\,\lambda_l \sin\,\delta_s + \cos\,\lambda_l \cos\,\delta_s \cos\left[\frac{2\pi(t_h - 12)}{24}\right] \tag{A2}$$

and thus the solar zenith angle $\theta_s = \pi/2 - \beta_s$. In Eq. (A2) t_h is local solar time (hours), λ_l is the latitude and δ_s is the declination of the sun with respect to the equator for day of year t_d:

$$\sin\,\delta_s = -\sin\left(\frac{23.45\pi}{180}\right)\cos\left(\frac{2\pi(t_d + 10)}{365}\right) \tag{A3}$$

Finally,

$$\cos\,\psi = \sin\theta \sin\,\psi + \cos\theta \cos\,\psi\cos(\alpha_s - \alpha) \tag{A4}$$

where θ is the zenith angle for the inclined surface and α and α_s are the azimuth angles of the surface and the sun, respectively. The latter is calculated using

$$\sin\,\alpha_s = \frac{-\sin\left[15\pi(12 - t_h)/180\right]\cos\delta_s}{\cos\beta_s} \tag{A5}$$

References

Aubinet, M., Vesala, T., Papale, D. (Eds.), 2011. Eddy Covariance: A Practical Guide to Measurement and Data Analysis. Springer Atmospheric Sciences.
Baldocchi, D., Falge, E., Gu, L.H., Olson, R., Hollinger, D., Running, S., Anthoni, P., Bernhofer, C., Davis, K., Evans, R., Fuentes, J., Goldstein, A., Katul, G., Law, B., Lee, X.H., Malhi, Y., Meyers, T., Munger, W., Oechel, W., Pilegaard, U.K.T.P., Schmid, K., Valentini, H.P., Verma, R., Vesala, S., Wilson, T., Wofsy, K.S., 2001. Fluxnet: a new tool to study the temporal and spatial variability of ecosystem-scale carbon dioxide, water vapor, and energy flux densities. Bull. Am. Meteorol. Soc. 82, 2415–2434.
Blanken, P.D., Black, T.A., Yang, P.C., Neumann, H.H., Nesic, Z., Staebler, R., den Hartog, G., Novak, M.D., Lee, X., 1997. Energy balance and canopy conductance of a boreal Aspen forest: partitioning overstory and understory components. J. Geophys. Res. Atmos. 102, 28915–28927.
Blonquist, J.M., Tanner, B.D., Bugbee, B., 2009. Evaluation of measurement accuracy and comparison of two new and three traditional net radiometers. Agric. For. Meteorol. 149, 1709–1721.
Brotzge, J.A., Duchon, C.E., 2000. A field comparison among a domeless net radiometer, two four-component net radiometers, and a domed net radiometer. J. Atmos. Ocean. Technol. 17, 1569–1582.
Buchan, G.D., 1989. Soil heat flux and soil surface energy balance: a clarification of concepts heat and mass transfer: Fourth Australasian Conference on heat and Mass Transfer , Christchurch, New Zealand, pp. 627–634.
Burba, G., Anderson, D., 2010. A Brief Practical Guide to Eddy Covariance Flux Measurements: Principles and workflow examples for scientific and industrial applications. http://www.licor.com/env/applications/eddy_covariance/book.jsp.
Clement, R.J., Burba, G.G., Grelle, A., Anderson, D.J., Moncrieff, J.B., 2009. Improved trace gas flux estimation through IRGA sampling optimization. Agric. For. Meteorol. 149, 623–638.
Finnigan, J.J., 1999. A comment on the paper by Lee (1998): on micrometeorological observations of surface-air exchange over tall vegetation. Agric. For. Meteorol. 97, 55–64.
Finnigan, J.J., 2004. A re-evaluation of long-term flux measurement techniques. Part II. Coordinate systems. Boundary Layer Meteorol. 113, 1–41.
Finnigan, J.J., Clement, R., Malhi, Y., Leuning, R., Cleugh, H.A., 2003. A re-evaluation of long-term flux measurement techniques. Part 1. Averaging and coordinate rotation. Boundary Layer Meteorol. 107, 1–48.
Foken, T., 2008. The energy balance closure problem: an overview. Ecol. Appl. 18, 1351–1367.
Foken, Th., Wichura, B., 1996. Tools for quality assessment of surface-based flux measurements. Agric. For. Meteorol. 78, 83–105.
Franssen, H.J.H., Stockli, R., Lehner, I., Rotenberg, E., Seneviratne, S.I., 2010. Energy balance closure of eddy-covariance data: a multisite analysis for European Fluxnet stations. Agric. For. Meteorol. 150, 1553–1567.
Fuchs, M., Tanner, C.B., 1968. Calibration and field test of soil heat flux plates. Soil Sci. Soc. Am. J. 32, 238–326.
Gao, Z., Horton, R., Liu, H.P., 2010. Impact of wave phase difference between soil surface heat flux and soil surface temperature on soil surface energy balance closure. J. Geophys. Res. Atmos. 115, D16112, doi:10.1029/2009JD013278.
Goudriaan, J., van Laar, H.H., 1994. Modelling Crop Growth Processes. Kluwer Academic Publishers, Amsterdam.
Halldin, S., Lindroth, A., 1992. Errors in net radiometry - comparison and evaluation of 6 radiometer designs. J. Atmos. Ocean. Technol. 9, 762–783.
Harman, I.N., Finnigan, J.J., 2010. Flow over hills covered by a plant canopy: extension to generalised two-dimensional topography. Boundary Layer Meteorol. 135, 51–65.
Haslwanter, A., Hammerle, A., Wohlfahrt, G., 2009. Open-path vs. closed-path eddy covariance measurements of the net ecosystem carbon dioxide and water vapor exchange: a long-term perspective. Agric. For. Meteorol. 149, 291–302.
Haverd, V., Cuntz, M., Leuning, R., Keith, H., 2007. Air and biomass heat storage fluxes in a forest canopy: calculation within a soil vegetation atmosphere transfer model. Agric. For. Meteorol. 147, 125–139.
Heitman, J.L., Horton, R., Sauer, T.J., Ren, T.S., Xiao, X., 2010. Latent heat in soil heat flux measurements. Agric. For. Meteorol. 150, 1147–1153.
Heusinkveld, B.G., Jacobs, A.F.G., Holtslag, A.A.M., Berkowicz, S.M., 2004. Surface energy balance closure in an arid region: role of soil heat flux. Agric. For. Meteorol. 122, 21–37.
Ibrom, A., Dellwik, E., Flyvbjerg, H., Jensen, N.O., Pilegaard, K., 2007. Strong low-pass filtering effects on water vapour flux measurements with closed-path eddy correlation systems. Agric. For. Meteorol. 147, 140–156.
Jung, M., Reichstein, M., Bondeau, A., 2009. Towards global empirical upscaling of fluxnet eddy covariance observations: validation of a model tree ensemble approach using a biosphere model. Biogeosciences 6, 2001–2013.
Kaimal, J.C., Businger, J.A., 1963. A continuous wave sonic anemometer-thermometer. J. Appl. Meteorol. 2, 156–164.
Kaimal, J.C., Finnigan, J.J., 1994. Atmospheric Boundary Layer Flows: Their Structure and Management. Oxford University Press, New York, p. 289.
Kanda, M., Inagaki, A., Letzel, M.O., Raasch, S., Watanabe, T., 2004. LES study of the energy imbalance problem with eddy covariance fluxes. Boundary Layer Meteorol. 110, 381–404.
Katul, G., Finnigan, J.J., Poggi, D., Leuning, R., Belcher, S.E., 2006. The influence of hilly terrain on canopy-atmosphere carbon dioxide exchange. Boundary Layer Meteorol. 118, 189–216.
Kohsiek, W., Liebethal, C., Foken, T., Vogt, R., Oncley, S.P., Bernhofer, C., Debruin, H.A.R., 2007. The energy balance experiment EBEX-2000. Part III. Behaviour and quality of the radiation measurements. Boundary Layer Meteorol. 123, 55–75.
Kondo, F., Tsukamoto, O., 2008. Evaluation of the Webb correction on CO_2 flux by eddy covariance technique using open-path gas analyser over asphalt surface. J. Agric. Meteorol. (Jpn.) 64, 1–8.
Kustas, W.P., Prueger, J.H., Hipps, L.E., Hatfield, J.L., Meek, D., 1998. Inconsistencies in net radiation estimates from use of several models of instruments in a desert environment. Agric. For. Meteorol. 90, 257–263.
Lee, X., 1998. On micrometeorological observations of surface-air exchanges over tall vegetation. Agric. For. Meteorol. 91, 39–49.
Lee, X., Massman, W., Law, B. (Eds.), 2004. Handbook of Micrometeorology: A Guide for Surface Flux Measurements, Analysis. Kluwer Academic Publishers, Dordrecht, The Netherlands, pp. 119–132.
Leuning, R., 2007. The correct form of the Webb, Pearman and Leuning equation for eddy fluxes of trace gases in steady and non-steady state, horizontally homogeneous flows. Boundary Layer Meteorol. 123, 263–267.
Leuning, R., Cleugh, H.A., Zegelin, S., Hughes, D., 2005. Carbon and water fluxes over a temperate Eucalyptus forest and a tropical wet/dry savanna in Australia: measurements and comparison with MODIS remote sensing estimates. Agric. For. Meteorol. 129, 151–173.
Leuning, R., Denmead, O.T., Lang, A.R.G., Ohtaki, E., 1982. Effects of heat and water vapour transport on eddy covariance measurements of CO_2 fluxes. Boundary Layer Meteorol. 23, 209–222.
Leuning, R., Judd, M.J., 1996. The relative merits of open- and closed-path analysers for measurements of eddy fluxes. Global Change Biol. 2, 241–253.
Leuning, R., King, K.M., 1992. Comparison of eddy-covariance measurements of CO_2 fluxes by open- and closed-path CO_2 analysers. Boundary Layer Meteorol. 59, 297–311.

Leuning, R., Moncrieff, J., 1990. Eddy-covariance CO_2 flux measurements using open-path and closed-path CO_2 analysers - corrections for analyser water vapour sensitivity and damping of fluctuations in air sampling tubes. Boundary Layer Meteorol. 53, 63–76.

Lindroth, A., Molder, M., Lagergren, F., 2010. Heat storage in forest biomass improves energy balance closure. Biogeosciences 7, 301–313.

Liu, H.P., Peters, G., Foken, T., 2001. New equations for sonic temperature variance and buoyancy heat flux with an omnidirectional sonic anemometer. Boundary Layer Meteorol. 100, 459–468.

Mammarella, I., Launiainen, S., Gronholm, T., Keronen, P., Pumpanen, J., Rannik, U., Vesala, T., 2009. Relative humidity effect on the high-frequency attenuation of water vapor flux measured by a closed-path eddy covariance system. J. Atmos. Ocean. Technol. 26, 1856–1866.

Massman, W.J., 1991. The attenuation of concentration fluctuations in turbulent-flow through a tube. J. Geophys. Res. 96, 5269–5273.

Massman, W.J., 1993. Errors Associated with the combination method for estimating soil heat-flux. Soil Sci. Soc. Am. J. 57, 1198–1202.

Massman, W.J., 2000. A simple method for estimating frequency response corrections for eddy covariance systems. Agric. For. Meteorol. 104, 185–198.

Massman, W.J., 2004. Concerning the measurement of atmospheric trace gas fluxes with open- and closed-path eddy covariance systems: the WPL terms and spectral attenuation. In: Lee, X., Massman, W.J., Law, B.E. (Eds.), Handbook of Micrometeorology: A Guide to Surface Flux Measurements. Kluwer Academic Publishers, Dordrecht, The Netherlands, pp. 133–160.

Massman, W.J., Clement, R., 2004. Uncertainty in eddy covariance flux estimates resulting from spectral attenuation. In: Lee, X., Massman, W.J., Law, B.E. (Eds.), Handbook of Micrometeorology: A Guide to Surface Flux Measurements. Kluwer Academic Publishers, Dordrecht, The Netherlands, pp. 67–99.

Massman, W.J., Ibrom, A., 2008. Attenuation of concentration fluctuations of water vapor and other trace gases in turbulent tube flow. Atmos. Chem. Phys. 8, 6245–6259.

Matzinger, N., Andretta, M., van Gorsel, E., Vogt, R., Ohmura, A., Rotach, M.W., 2003. Surface radiation budget in an Alpine valley. Q. J. R. Meteorol. Soc. 129 (588), 877–895, doi:10.1256/qj.02.44.

Mauder, M., Oncley, S.P., Vogt, R., Weidinger, T., Ribeiro, L., Bernhofer, C., Foken, T., Kohsiek, W., De Bruin, H.A.R., Liu, H., 2007. The energy balance experiment EBEX-2000. Part II. Intercomparison of eddy-covariance sensors and post-field data processing methods. Boundary Layer Meteorol. 123, 29–54.

Meyers, T.P., Hollinger, S.E., 2004. An assessment of storage terms in the surface energy balance of maize and soybean. Agric. For. Meteorol. 125, 105–115.

Michel, D., Philipona, R., Ruckstuhl, C., Vogt, R., Vuilleumier, L., 2008. Performance and uncertainty of CNR1 net radiometers during a one-year field comparison. J. Atmos. Ocean. Technol. 25, 442–451.

Moore, C.J., 1986. Frequency response corrections for eddy correlation systems. Boundary Layer Meteorol. 37, 17–35.

Ochsner, T.E., Sauer, T.J., Horton, R., 2007. Soil heat storage measurements in energy balance studies. Agron. J. 99, 311–319.

Olmo, F.J., Vida, J., Foyo, I., Castro-Diez, Y., Alados-Arboledas, L., 1999. Prediction of global irradiance on inclined surfaces from horizontal global irradiance. Energy 24, 689–704.

Oncley, S.P., Foken, T., Vogt, R., Kohsiek, W., Debruin, H.A.R., Bernhofer, C., Christen, A., Van Gorsel, E., Grantz, D., Feigenwinter, C., Lehner, I., Liebethal, C., Liu, H., Mauder, M., Pitacco, A., Ribeiro, L., Weidinger, T., 2007. The energy balance experiment EBEX-2000. Part I: Overview and energy balance. Boundary Layer Meteorol. 123, 1–28.

Philip, J.R., 1961. The theory of heat flux meters. J. Geophys. Res. 66, 571–579.

Sauer, T.J., Horton, R., 2005. Soil heat flux. In: Hatfield, J.L., Baker, J.M., Viney, M.K. (Eds.), Micrometeorological Measurements in Agricultural Ecosystems. ASA, CSSA and SSA Monograph No. 47, Madison, Wisconsin, USA, pp. 131–154.

Schotanus, P., Niewstadt, F.T.M., De Bruin, H.A.R., 1983. Temperature measurements with a sonic anemometer and its application to heat and moisture fluxes. Boundary Layer Meteorol. 26, 81–93.

Spank, U., Bernhofer, C., 2008. Another simple method of spectral correction to obtain robust eddy-covariance results. Boundary Layer Meteorol. 128, 403–422.

Steinfeld, G., Letzel, M.O., Raasch, S., Kanda, M., Inagaki, A., 2007. Spatial representativeness of single tower measurements and the imbalance problem with eddy-covariance fluxes: results of a large-eddy simulation study. Boundary Layer Meteorol. 123, 77–98.

Stull, R.B., 1988. An Introduction to Boundary Layer Meteorology. Kluwer Academic Publishers, Dordrecht, The Netherlands.

Twine, T.E., Kustas, W.P., Norman, J.M., Cook, D.R., Houser, P.R., Meyers, T.P., Prueger, J.H., Starks, P.J., Wesely, M.L., 2000. Correcting eddy-covariance flux underestimates over a grassland. Agric. For. Meteorol. 103, 279–300.

van Gorsel, E., Harman, I.N., Finnigan, J.J., Leuning, R., 2011. Decoupling of air flow above and in plant canopies and gravity waves affect micrometeorological estimates of net scalar exchange. Agric. For. Meteorol. 151, 927–933.

van Gorsel, E., Leuning, R., Cleugh, H.A.K.H., Suni, T., 2007. Nocturnal carbon efflux: reconciliation of eddy covariance and chamber measurements using an alternative to the u_*-threshold filtering technique. Tellus Ser. B Chem. Phys. Meteorol. 59B, 397–403.

van Wijk, W.R., de Vries, D.A., 1963. Periodic temperature variations in a homogeneous soil. In: van Wijk, W.R. (Ed.), Physics of Plant Environment. North-Holland Publishing Co., Amsterdam, pp. 102–143.

Webb, E.K., Pearman, G.I., Leuning, R., 1980. Correction of flux measurements for density effects due to heat and water vapour transfer. Q. J. Roy. Met. Soc. 106, 85–100.

Wilczak, J.M., Oncley, S.P., Stage, S.A., 2001. Sonic anemometer tilt correction algorithms. Boundary Layer Meteorol. 99, 127–150.

Williams, M., Richardson, A.D., Reichstein, M., Stoy, P.C., Peylin, P., Verbeeck, H., Carvalhais, N., Jung, M., Hollinger, D.Y., Kattge, J., Leuning, R., Luo, Y., Tomelleri, E., Trudinger, C.M., Wang, Y.P., 2009. Improving land surface models with Fluxnet data. Biogeosciences 6, 1341–1359.

Wilson, K., Goldstein, A., Falge, E., Aubinet, M., Baldocchi, D., Berbigier, P., Bernhofer, C., Ceulemans, R., Dolman, H., Field, C., Grelle, A., Ibrom, A., Law, B.E., Kowalski, A., Meyers, T., Moncrieff, J., Monson, R., Oechel, W., Tenhunen, J., Valentini, R., Verma, S., 2002. Energy balance closure at Fluxnet sites. Agric. For. Meteorol. 113, 223–243.

Yi, C.X., Anderson, D.E., Turnipseed, A.A., Burns, S.P., Sparks, J.P., Stannard, D.I., Monson, R.K., 2008. The contribution of advective fluxes to net ecosystem exchange in a high-elevation, subalpine forest. Ecol. Appl. 18, 1379–1390.